The Airborne Millimeter-wave System Development and Performance Update for NCAR's HAIPER Cloud Radar

Pei-Sang Tsai*, **E. Loew, S. Ellis, J. Vivekananadan, J. Emmett, C. Burghart, S. Rauenbuehler, M. Dixon, M. Strong**
Earth Observing Laboratory, National Center for Atmospheric Research, Boulder, Colorado
S. Haimov
Department of Atmospheric Science, University of Wyoming, Wyoming

1. Introduction

The High-Performance Instrumented Airborne Platform (HIAPER) is a National Science Foundation (NSF) funded aircraft which supports environmental research. It is a high-altitude, long-endurance Gulfstream V aircraft designed to house a suite of in situ and remote sensing instruments. The Earth Observing Laboratory (EOL) is currently developing a scanning, W-band cloud radar mounted in a wing pod on the HIAPER aircraft (1; 2). The phased approach in designing and developing the so-called HIAPER Cloud Radar (HCR) includes the following steps: the initial ground-based, proof-of-concept prototype; the airborne configuration; dual-polarized, pulse compression airborne system and, the final stage, dual wavelength (W- and Ka-band) system(3).

The HCR was transitioned into the airborne configuration in 2012. Several intermediate engineering validations were conducted to evaluate the HCR performance: ground validation of the pod-based airborne system (4), integration with the HIAPER aircraft and finally, flight validation during a test flight in February 2013.

This paper describes the progress of HCR development including aircraft integration, calibration, and radar performance. The preliminary ground-based intercomparison with the Wyoming Cloud Radar (WCR) showed the two systems were in good agreement. Preliminary data from the test flights are included to demonstrate the airborne system performance. The high-altitude, aircraft exterior environmental data are used to examine the system stability.

*Corresponding author address: Pei-Sang Tsai, Earth Observing Laboratory, National Center for Atmospheric Research, Boulder CO 80301, E-mail: ptsai@ucar.edu

2. Airborne Flight Test

HCR airborne configuration was integrated to HIAPER aircraft for the SANNGRIA-TEST flight deployments in February 2013. The deployment includes five six-hour, 40,000 ft, night-time flights and one INS calibration flight. The INS calibration maneuvers were carried out over flat terrain and low vegetation (Kansas) to estimate the ground echo velocity(5).

a. *Real-time System Monitoring*

To better understand HCR's underwing, pod environment, extensive engineering effort has been devoted to a real-time environmental monitoring. A total of thirteen temperature sensors and two pressure sensors are installed on various key components of the receiver. System status, states of the control signals, along with all the sensor feedbacks are recorded in the archived dataset. Figure 2 demonstrates the temperature time series for a typical test flight. With this detailed information, radar performance such as receiver gain variation, transmit peak power, and receiver sensitivity can be closely observed.

An infrastructure monitoring software application was implemented within the HCR real-time visualization tool-

Figure 1: HCR installed on NCAR GV aircraft. Front large pod: HIAPER Cloud Radar; rear large pod: counter weight.

box. This software application allows the operator to monitor each signal through time. It alerts the operator of any minor to critical errors in a timely manner. It also provides a real-time snapshot of the entire system status. This real-time environmental, system monitoring will help achieve HCR's future remote operation goals.

b. *Electromagnetic Interference*

The radar system is required to be compliant with Federal Aviation Administration (FAA) regulations to be part of GV's instrumentation. Regulations include the use of certified electrical wires, mounting fixtures, and the construction of the electrical system. In order to be flight-certified, HCR was integrated to GV to ensure its compatibility. Tests included: electrical continuity, mechanical structure support, aircraft power supply interference to radar system, and electromagnetic interference to aircraft communication.

FAA requires all payload instrumentation to be free of interference between 108 to 136 MHz to ensure aviation safety. HCR is free of electromagnetic interference at various radar intermediate frequencies except for VHF band, namely, 125 MHz. The main source of the VHF interference was detected in the vicinity of the aircraft py-

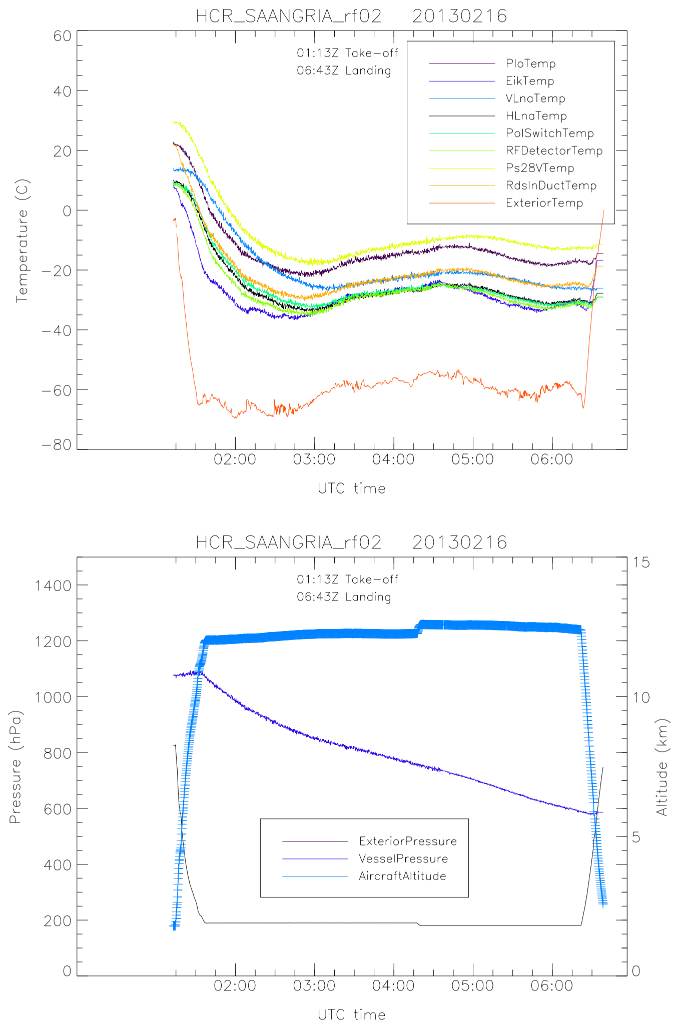

Figure 2: Time series of all on-board sensors during research flight on February 16th, 2013. Top: temperature sensors; Bottom: aircraft altitude, exterior pressure and HCR internal vessel pressure. Vessel pressure leakage is approximately 3.15 psi/hr.

Figure 3: 125 MHz interference to aircraft communication is the high-data-rate Gigabit Ethernet cables located in the pylon.

lon. Signals such as digitized radar returns, Ethernet, control signals, environmental status, fiber optics and radar STALO travels through the pylon structure to the fuselage operator station. The bundled signal cables as shown in Figure **??**fig:emi, handle high-capacity communication and the limited space inside the pylon makes electromagnetic shielding a challenge. The final source of interference was identified to be the gigabit Ethernet cables. The interference was reduced down to the level of a minor annoyance, insignificant to interrupt air traffic communications.

c. *System Pressurization and Temperature*

To accommodate GV's wide range of flight altitudes, a pressurized, 13-inch, cylindrical chamber was designed to house the radar electronics. The chamber is sealed and pressurized to 20 psia (1896 hPa) at ground level prior to each flight. Additional pressure, approximately 8 psi above ground level, provides a buffer to temperature fluctuation and leakage from a non-ideal mechanical design. High voltage electronics such as the transmitter power supply, requires a minimum of 11.32 psia (780.3 hPa) pressure for normal operation. However, the fixed amount of air molecules in the chamber provides limited air circulation for system cooling. Therefore, an efficient conduction cooling mechanism is designed to dissipate heat through the chamber floor. The excess heat is conducted to the longitudinal, finned, heat sink on the other side of the floor. The exterior air, ducted from the bottom of the pod, exchanges the heat load and exhausts at the tail of the pod.

For SAANGRIA-TEST flights, GV maintained a constant, 40,000 ft cruising altitude. Figure 2 top figure illustrates temperature measurements during a research flight on February 16th, 2013. For an exterior air temperature of around -70 $^\circ$C, the HCR temperature was around -40 $^\circ$C during flight.

The effective conduction cooling puts the system below desired operating temperature for winter, high altitude flights. The exterior air duct was closed and an insulating layer was installed between the aircraft pod and the pressure chamber. Compared to Figure 2, top figure 4 shows overall temperature improvement from the two adjustments. The adjustments successfully raised the overall temperature above 0 $^\circ$C. The system temperature improvements not only increased the radar system stability but also reduced the pressure leak rate during flights.

3. System Performance Analysis

a. *Receiver Stability*

Under such extreme in-flight temperature conditions, the receiver stability was investigated. Figure 5 shows the receiver noise floor fluctuation versus system temperature. The noise floor shows an inverse correlation with temperature. The variation can be has large as 2.06 dB. The transmit peak power was also affected by ambient temperature. Approximately 45 minutes of unstable warm-up period was observed. About 3 dB of peak power variation is also contributed from the environmental effects. The 2 dB in receiver noise floor will directly affect system sensitivity by the equal amount. The transmit peak power fluctuation also poses the same effect. To optimize the maximum sensitivity, it is not only essential to increase the overall system temperature but to minimize the temperature fluctuation. More environmental analysis will be perform to identify the optimum operating temperature of the HCR pod.

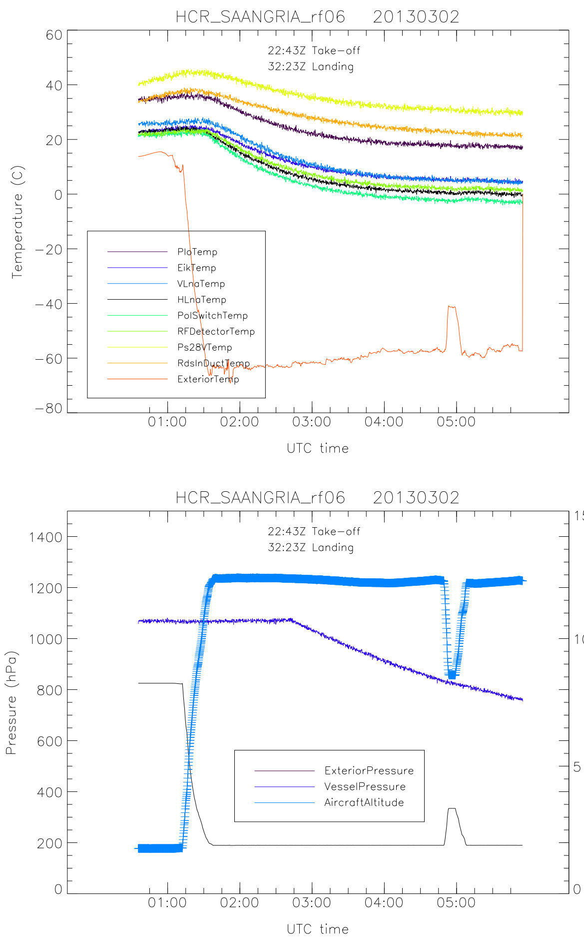

Figure 4: Top: temperature time series after the installation of insulation layer and reduced duct air flow. Bottom: Aircraft altitude and corrected exterior pressure. Vessel pressure leak rate equates to 2.78 psi/hr.

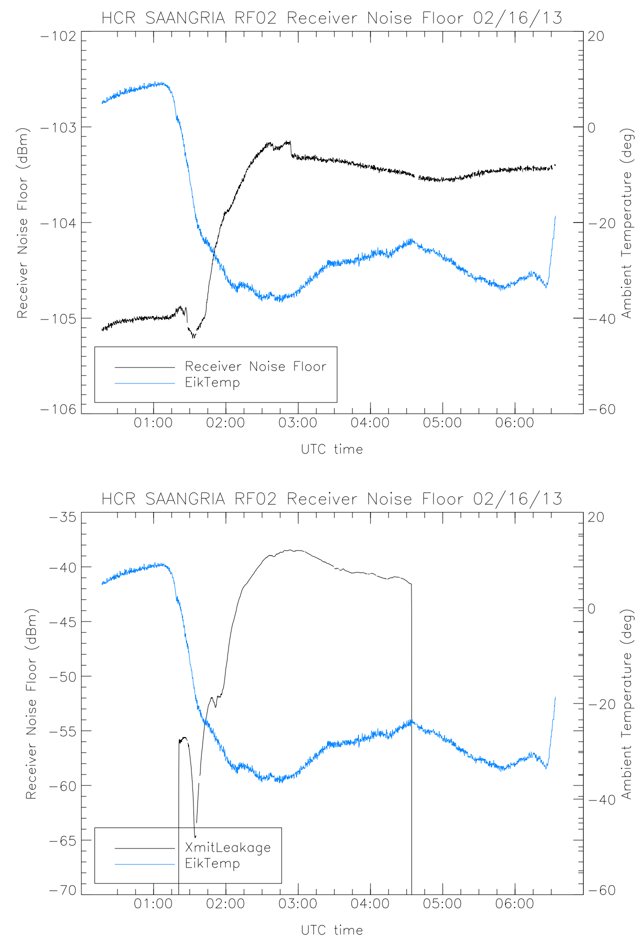

Figure 5: HCR receiver stability. Top: receiver noise floor fluctuation versus system temperature; bottom: transmitter peak power versus temperature.

Table 1: WCR/HCR operating parameters during intercomparison.

$Parameters$	HCR	WCR
Pulse Width	256 ns	250 ns
Dwell Time	162 m	160 m
Range Resolution	38.4 m	37.5 m
Max. Range	8.9 km	9.3 km
Elevation Angle	30.6 deg	30.6 deg

b. *Cloud Observations*

A sample cloud obseravation is shown in Figure 6. A minimum reflectivity -35 dBZ was observed in the dataset (left figure). Basic noise correction was applied with a received power threshold at -98.25 dBm. The strong reflection around 250 m altitude represents the ground echo. The velocity (right figure) was corrected using HCR in-pod INS navigation data. A mean velocity of the ground after correction is approximately -0.0024 m/s (5).

4. Wyoming Cloud Radar Intercomparison

HCR was brought to University of Wyoming for a collaborative engineering assessment. By comparing with the well-calibrated, mature Wyoming Cloud Radar (WCR), deficiencies and performance of HCR could be easily verified. With comparable radar specification such as wavelength, transmit power, beamwidth and receiver gain, both radars are expected to have similar performance. Due to the radar platform limitation, both radar systems were set up inside the hangar, pointing southwards (Figure 7). WCR was set up on a rotatable platform. The elevation angle of HCR was achieved by manually adjusting the rotatable reflector. To minimize the error from operation, the computer times were synchronized within 1 second. Both radar were operated with comparable operational parameters listed in Table 1.

Cloud Observation

A 30-minute stratiform rain event was observed by both radars on September 27, 2012. To accurately evaluate the performance, minimum time and range interpolation was performed on WCR data. The preliminary, aligned signal-to-noise ratio(SNR) from both systems are shown in Figure 8. Similar patterns are recorded in both systems.

5. Summary

This paper summarizes the engineering challenges and performance of the HIAPER cloud radar during its first test flights and in comparison with WCR. The preliminary analysis of measurements shows good agreement between WCR and HCR measurements. The flight data and environmental analysis indicates good radar sensitivity and attitude correction (5). The radar system still faces several engineering challenges in stabilizing the system temperature to achieve high sensitivity and receiver gain and minimizing pressure leakage to prolong its flight time. HCR is currently participating in IDEAS-V deployment for its second test flights. Deficiencies discovered during SAANGRIA-TEST flights have been addressed and will be tested again during this deployment.

Acknowledgement The National Center for Atmospheric Research is sponsored by the National Science Foundation under American Recovery and Reinvestment Act (ARRA) Grant Number M0904552.

References

[1] J. Moore, J. Vivekanandan, et al.. *Development of Advanced Radar and Lidar Platform Suite for Interdisciplinary Airborne and Ground-based Remote Sensing Research*. In *Proc. of 33th Conf. on Radar Meteorology, 2007*, P8B.10.

[2] J. Vivekanandan, E. Loew, et al. *Ground-based and Airborne Weather Radars and Lidar for Observing the Atmosphere*. In *Proc. of 34th Conf. on Radar Meteorology, 2009*, 12B.3.

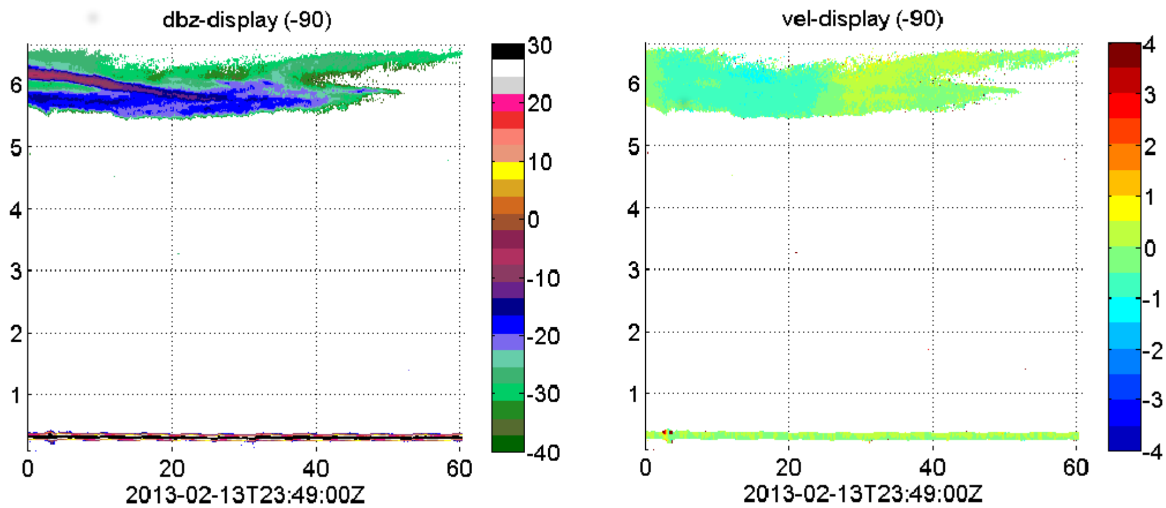

Figure 6: A sample cloud observation on February 13th, 2013. Left: reflectivity (dBZ); right: Velocity (m/s).(5)

Figure 7: WCR/HCR intercomparison setup. WCR (right) mounted on an adjustable platform for elevation angles. HCR (left) stationary-positioned with a manual rotatable reflector. A microwave absorber panel was placed between both radars to minimize interference.

[3] G. Farquharson, E. Loew, J. Vivekanandan, et al. *A New High-altitude Airborne Millimeter-wave Radar for Atmosphere Research*. In *Proc. of 33th Conf. on Radar Meteorology, 2007*, P8B.5.

[4] P. Tsai, E. Loew, J. Vivekanandan, et al. *NCAR HIAPER Cloud Radar Design and Development*. In *Proc. of 35th Conf. on Radar Meteorology, 2011*, P12.193.

[5] S. Ellis, J. Vivekanandan, et al. *Initial Evaluation of the HIAPER Cloud Radar Doppler Velocity Measurements*. In *Proc. of 36th Conf. on Radar Meteorology, 16-20 September 2013*, 8A.6.

[6] R. J. Doviak and D. S. Zrnić. *Doppler Radar and Weather Observations*. Academic Press, second edition, 1993.

[7] B. E. Martner,K. A. Clark, B. W. Bartram Radar Calibration Using a Trihedral Corner Reflector *Repr. fo 31st Conf. on Radar Meteorology*, page 1028-1030

[8] F. T. Ulaby, R. K. Moore, A. K. Fung Microwave Remote Sensing, Active and Passive *Artech House, Inc.*, Volume II, 1986

[9] M. I. Skolnik Introduction to Radar Systems *McGraw Hill Pub.*, third Edition, 2001

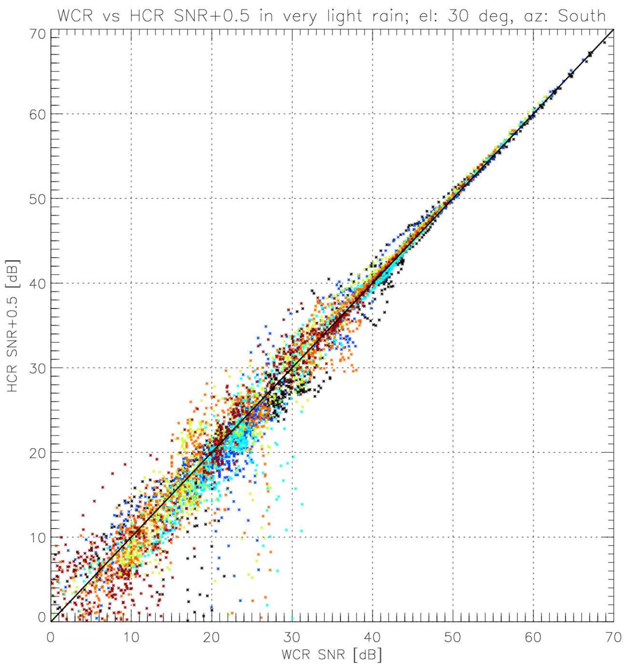

Figure 8: WCR/HCR signal-to-noise ratio scatter plot.

[10] Texas Instruments. *Understanding Data Converters*, 1995. Application Report.